Experimental investigation on bit-rate-adaptive software synchronous optical sampling

Lin Zuo (左 林), Lihui Feng (冯立辉)*, Aiying Yang (杨爱英), Junsen Lai (赖俊森), and Yunan Sun (孙雨南)

School of Optoelectronics, Beijing Institute of Technology, Beijing 100081, China

**Corresponding author: lihui.feng@bit.edu.cn*

Received November 12, 2012; accepted January 25, 2013; posted online April 24, 2013

A tunable optical rail is embedded into the cavity of a nonlinear-polarization-rotation (NPR) mode-locked fiber laser to generate a sampling pulse with different repetition frequencies and realize bit-rate-adaptive software synchronous optical sampling. Two ultrashort pulses (20.26677 and 20.22900 MHz) are derived, and a 100-MHz data signal is sampled twice with these pulses based on sum-frequency generation (SFG) in periodically poled lithium niobate (PPLN). The eye diagram is successfully recovered, and an estimated bit rate of 102.22 MHz is derived. This method is feasible for bit rates ranging from 200 MHz to 1 GHz, with <3% relative error.

OCIS codes: 060.4370, 190.4360, 070.4340.

doi: 10.3788/COL201311.050603.

The rapid development of wavelength-division multiplexing (WDM) networks has enabled successful investigations on transmission rates of more than 40 Gb/s per channel, and various novel modulation formats are emerging. Therefore, optical performance monitoring (OPM) has become an urgent need to obtain network parameters and ensure the normal operation of optical communication. However, traditional electric access to data signals is becoming increasingly complicated because of the electric speed bottleneck. Therefore, all optical solutions for performance monitoring have become promising. Compared with synchronous or asynchronous optical sampling[1], the software synchronous optical sampling technique can conveniently provide the quality factor and eye diagram in real time, requiring no timing clock for sampling pulses. Thus, this technique is an effective method of OPM. A software algorithm for deriving timing information hidden in a seemingly unordered sampled signal has been introduced[2,3], and an eye diagram has been recovered. A software synchronous optical sampling technique based on periodically poled lithium niobate (PPLN)[4] or highly nonlinear optical fiber[5] has also been reported. Furthermore, a study[6] using a sampling pulse with two different repetition frequencies theoretically recovers the bit rate of the data signal and indicates that the software synchronous optical sampling technique can be bit-rate transparent, which has significant meaning in practical applications.

This letter introduces the principle of the bit-rate-adaptive software synchronous optical sampling technique and reports the relevant experimental investigation performed. With an optical rail embedded in the ring cavity, a nonlinear-polarization-rotation (NPR) mode-locked fiber laser generates an ultrashort pulse and the repetition frequency is tuned. Two ultrashort pulses (20.26677 and 20.22900 MHz) are used to sample a 100-MHz optical data signal successively based on the sum-frequency generation (SFG) process in PPLN. The accurate number of scanned bit slots is calculated, the eye diagram is recovered, and an estimated bit rate of 102.22 MHz is successfully derived. For a data signal with bit rates ranging from 200 MHz to 1 GHz, the error of the recovered bit rate relative to the real value does not exceed 3%.

Figure 1 shows the setup of software asynchronous optical sampling with the bit-rate-adaptive method. A mode-locked laser (MLL), which is discussed in detail later, is used to generate the sampling pulse with frequencies f_{s1} and f_{s2}. The data signal to be sampled has a bit rate represented by B and is simply formed by modulating a wavelength tunable continuous wave (CW) with a sinusoidal radio-frequency (RF) signal. The sampling pulse and data signal are joined together by a coupler and sent into the sampling device, which serves as the nonlinear AND gate controlled by the sampling pulse. PPLN is used as the sampling device, and optical sampling is accomplished by the SFG process with the advantage of ultra fast response time. The sampled optical data signal is detected by a low bandwidth photon detector (PD), converted into a digital signal by the data acquisition circuit, and finally analyzed by a computer to recover timing information and establish an eye diagram.

For an N-point-long sampled data stream X, the mean-square transform is performed firstly as

$$Y_i = \left(X_i - \overline{X}\right)^2, \tag{1}$$

where $\overline{X}$ is the mean value of N points. Applying Fourier transform to Y yields the spectrum component corresponding to the peak value S', i.e., the coarse number of the scanned bit slots. S' is inaccurate because of the resolution limitation of the Fourier transform; thus, chirped Z transform (CZT) is needed to improve the precision

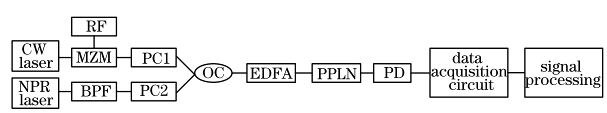

Fig. 1. Setup of the software asynchronous optical sampling technique. MZM: Mach–Zehnder modulator; PC: polarization controller; BPF: band pass filter; OC: optical coupler; EDFA: erbium-doped fiber amplifier.

 © 2013 Chinese Optics Letters

and determine the accurate number of scanned bit slots $S^{[7]}$. Finally, the eye diagram with bit number as time axis is reconstructed using S and $N^{[8]}$.

The relationship among S, B, N, and f_s is investigated as follows. The integer component of the ratio of B to f_s is the frequency reduction factor M given by $M = \lfloor B/f_s \rfloor$, where $\lfloor x \rfloor$ is an integer not larger than x. The offset frequency Δf is calculated as $B = Mf_s + \Delta f$, which is written in the time domain as $1/f_s = M/B + \mathrm{d}t$, where $\mathrm{d}t$ is the equivalent time step. Considering that $S = \mathrm{d}t \cdot N \cdot B^{[2]}$, the equation $M = B/f_s - S/N$ is derived. If f_{s1} and f_{s2} are appropriately chosen to satisfy $M_1 = M_2$ or $B/f_{s1} - S_1/N_1 = B/f_{s2} - S_2/N_2$, then B is derived by

$$B = \left| \frac{S_1/N_1 - S_2/N_2}{1/f_{s1} - 1/f_{s2}} \right|. \quad (2)$$

Bit-rate adaption is realized because S, B, and f_s are determined without prior knowledge of the bit rate or modulation format. A necessary condition to meet $M_1 = M_2$ is $|1/f_{s1} - 1/f_{s2}| \leqslant 1/B$, which can be used to estimate the range of B that can be correctly recovered with the given f_{s1} and f_{s2}. For example, if f_{s1}=20.26677 MHz and f_{s2} = 20.22900 MHz, the result shows that this method is applicable for B values lower than 10 Gb/s. A lower discrepancy between f_{s1} and f_{s2} can also be deduced to lead to a wider range of B.

The MLL is the most commonly used sampling source. Varying the frequency of the pulse by tuning the frequency of an imposed external modulation signal is convenient for an active MLL. However, no external modulation signal exists for a passive MLL. According to the formula $f = c/(nL)$, where c is the speed of light and n is the refraction index, the repetition frequency f is inversely proportional to the length of the ring cavity L. Therefore, varying the cavity length is a commonly used method to change the repetition frequency[9] because this method is cost effective and easy.

In this letter, a NPR passive MLL[10] is used with an optical rail embedded in a cavity, as shown in Fig. 2. Two collimators are fixed on the optical rail, and the

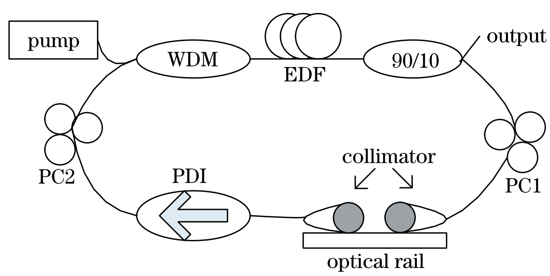

Fig. 2. Schematic of the NPR mode-locked fiber laser.

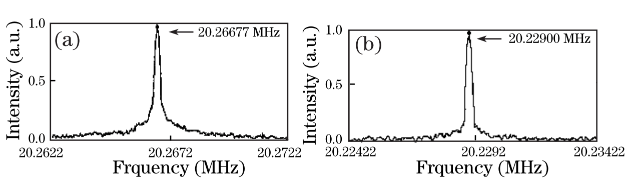

Fig. 3. Fundamental frequency of a mode-locked pulse measured using a spectrum analyzer: (a) 20.26677 and (b) 20.22900 MHz.

distance between them can be tuned by adjusting the coarse and fine tuning knobs.

The wavelength of the pump light is 980 nm and the power is 193 mW. Mode-locked pulse strings with repetition frequencies f_{s1} = 20.26677 MHz and f_{s2} = 20.22900 MHz are derived when the distance between collimators differs. The corresponding RF spectrum is shown in Fig. 3. Notably, when the distance between two collimators varies, collimators and polarization controllers (PCs) should be readjusted to ensure time-stable mode-locked pulses. Readjustment is performed because of the precision limitation of the optical rail, i.e., collimators are no longer precisely aligned when they are tuned. The insertion loss correspondingly increases and disturbs the polarization states of mode-locked pulses. However, the central wavelength only slightly changes because the PC adjustment is minimal. Figure 4 shows the optical spectrum, which indicates that the central wavelength for both states is about 1 560 nm even though the two optical spectra have different shapes. In addition, the sideband indicates that both spectra are traditional soliton pulses.

A 30-mm-long 5-mol% MgO-doped PPLN waveguide (HC Photonics, Taiwan) with a quasi-phase-matching (QPM) grating period of 19.3 μm is used. The PD (PDA10A, Thorlabs, USA) comprises a Si PIN detector (wavelength range: 200-1 100 nm) with an amplifying circuit for detecting weak SFG signals. In the first experiment, the frequency of the sampling pulse is f_{s1} = 20.26677 MHz, whereas the frequency of the RF signal is 100 MHz. The band pass filter (BPF, Alnair Labs Corp, Japan) has an insertion loss of less than 5 dB and a wavelength that can be tuned from 1 530 to 1 570 nm, covering the C band. The spectral bandwidth is also tunable, ranging from 14.5 to approximately 0 nm.

As shown in Fig. 5, the wavelength of the CW laser is 1 544.85 nm and the central wavelength of BPF is tuned to be 1 556.20 nm to meet the QPM condition. The bandwidth of BPF is 0.35 nm, the temperature of PPLN is fixed at 61.5 °C, and the output power of the erbium-doped fiber amplifier (EDFA) is 8.70 dBm. The measured optical spectrum of SFG light is shown in Fig. 6 with a peak power of –26.06 dBm. The sampled data stream X with a length of N_1 = 1 024 is converted into digital format using a PD and a 14-bit analog-to-digital converter. The algorithm introduced above is then adopted to obtain the result of CZT to Y, as depicted in Fig. 7(a). The corresponding S_1 is 67.3872, which is very close to the theoretically calculated value of 67.3942. The eye diagram of the sinusoidal data signal is successfully recovered based on the results, as shown in Fig. 8.

The sampling pulse frequency is changed to f_{s2} = 20.22900 MHz, whereas the other parameters including N_2 = 1 024 are fixed. Given that the optical spectrum of sampling pulse, data signal, SFG light, and the recovered eye diagram are similar to the results obtained when f_{s1} = 20.26677 MHz, their figures are not presented for brevity. However, the S_2 value obtained is 57.7443 (Fig. 7(b)), which is close to the calculated value of 57.9604.

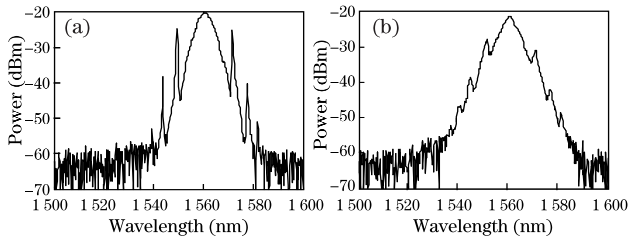

Fig. 4. Optical spectra of mode-locked pulse with frequencies of (a) 20.26677 and (b) 20.22900 MHz.

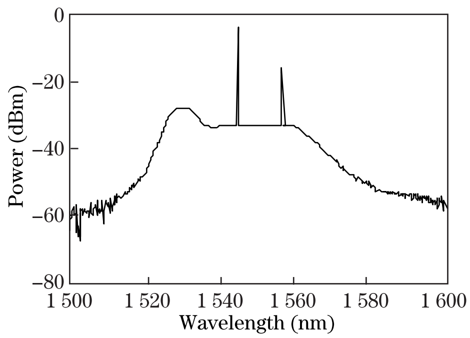

Fig. 5. Optical spectrum of data signal and sampling pulse amplified by the EDFA. The peak at 1 544.85 nm is the data signal, and the peak at 1 556.20 nm is the sampling pulse.

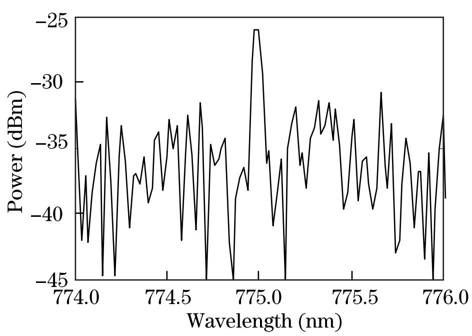

Fig. 6. Optical spectrum of SFG light (peak at 775 nm).

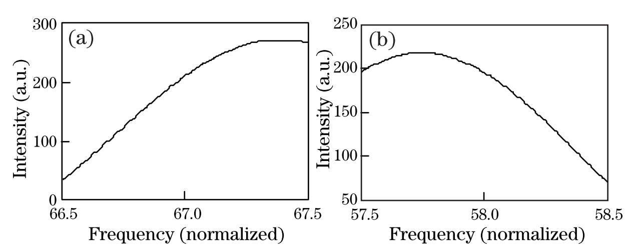

Fig. 7. CZT results of sampled data with (a) 20.26677 and (b) 20.22900 MHz sampling pulses. The frequency component corresponding to the peak is S.

The frequency reduction factor is 4 for both f_{s1} and f_{s2}; thus, they can be used to recover the bit rate. According to Eq. (2), the recovered value for B is 102.22 MHz, which well coincides well with its real value of 100 MHz. The maximum RF signal frequency is 1 GHz because of the performance limitation of the RF source. The corresponding recovered bit rates for another 40 different RF frequencies ranging from 1 MHz to 1 GHz are plotted as circles in Fig. 9, and the real values are presented as a solid line.

The error of the recovered bit rate relative to its real value ($\Delta B/B$) is presented as a dotted line in Fig. 9. The error in software synchronous sampling is attributed to the relatively higher error of the calculated S when the decimal part of B/f_s (i.e., $B/f_s - \lfloor B/f_s \rfloor$) approaches 0 or 1. Assuming that $N_1 = N_2 = N$ and based on Eq. (2), the recovered bit rate is expressed as

$$\Delta B = \frac{f_{s1} f_{s2}}{N\,|f_{s2} - f_{s1}|} \Delta\,|S_1 - S_2|\,. \tag{3}$$

The relation between $\Delta\,|S_1 - S_2|$ (i.e., the absolute error of $|S_1 - S_2|$) and B obtained by numerical simulation is shown in Fig. 10. For point A, $B = 527$ MHz and $B/f_{s1} - \lfloor B/f_{s1} \rfloor = 0.003$; for point B, $B = 445$ MHz and $B/f_{s2} - \lfloor B/f_{s2} \rfloor = 0.998$. However, from a statistical perspective, $\Delta\,|S_1 - S_2|$ is not related with B and ΔB according to Eq. (3). Thus, we conclude that $\Delta B/B$ generally decreases with increased B, as confirmed in

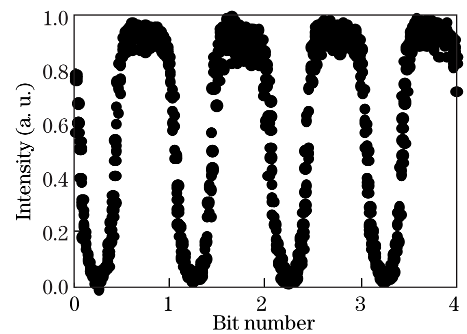

Fig. 8. Recovered eye diagram of the 100-MHz sinusoidal signal.

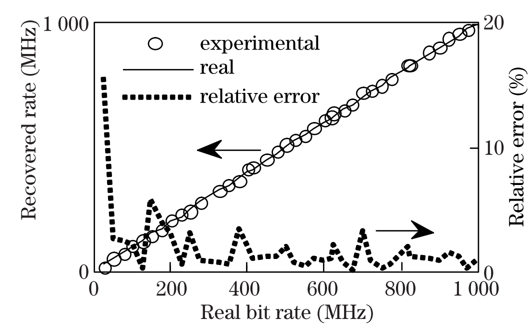

Fig. 9. Recovered bit rate and the relative error.

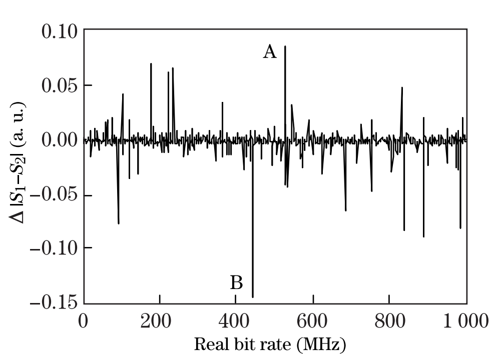

Fig. 10. Relationship between $\Delta\,|S_1 - S_2|$ and B.

Fig. 9. For bit rates more than 200 MHz, the error relative to the true value does not exceed 3%, which demonstrates the feasibility of bit rate adaptive software synchronous optical sampling.

In conclusion, with an optical rail embedded in the ring cavity, a NPR mode-locked fiber laser generates an ultrashort pulse with repetition frequencies of 20.26677 and 20.22900 MHz. A 100-MHz optical data signal is then sampled twice with these frequencies based on the SFG process in PPLN, where the power of SFG light is –26.06 dBm. The accurate numbers of scanned bit slots are calculated to be 67.3872 and 57.7443, which are very close to the theoretical values of 67.3942 and 57.9604, respectively. The eye diagram is recovered, and an estimated bit rate of 102.22 MHz is successfully derived. For data signals with bit rates ranging from 200 MHz to 1 GHz, the error of the recovered bit rate relative to the real value does not exceed 3%. For a future sampled data stream, more points should be recorded to achieve better precision. Bit rates of up to 10 GHz can also be recovered using an improved RF transmitter.

This work was supported by the National Natural Science Foundation of China (Nos. 60978007, 61027007, and 61177067) and the Open Fund of Key Laboratory of Optical Communication and Light wave Technologies, Beijing University of Posts and Telecommunications, Ministry of Education, China.

References

1. H. Y. Choi, Y. Takushima, and Y. C. Chung, Opt. Express **17,** 23953 (2009).
2. M. Westlund, H. Sunnerud, M. Karlsson, and P. A. Andrekson, J. Lightwave Technol. **23,** 1088 (2005).
3. A. Y. Yang, X. Y. Wu, and Y. N. Sun, Chin. Opt. Lett. **7,** 194 (2009).
4. M. T. Liu, A. Y. Yang, and Y. N. Sun, Acta Opt. Sin. (in Chinese) **28,** 283 (2008).
5. D. K. Tang, J. G. Zhang, Y. S. Liu, and W. Zhao, Chin. Opt. Lett. **8,** 630 (2010).
6. A. Y. Yang, X. Y. Wu, Y. J. Qiao, and Y. N. Sun, Opt. Commun. **284,** 436 (2011).
7. A. Y. Yang, J. S. Lai, and Y. N. Sun, IEEE Photon. Technol. Lett. **23,** 1739 (2011).
8. J. Li, A. Y. Yang, L. Zuo, J. S. Lai, and Y. N. Sun, Front. Optoelectron. **5,** 208 (2012).
9. J. Chen, J. W. Sickler, E. P. Ippen, and F. X. Kartner, Opt. Lett. **32,** 1566 (2007).
10. Z. C. Luo, W. C. Xu, C. X. Song, A. P. Luo, and W. C. Chen, Chin. Phys. B **18,** 2328 (2009).